Journal of the European Ceramic Society 22 (2002) 1183–1189

www.elsevier.com/locate/jeurceramsoc

# Instrumented indentation test for advanced technical ceramics

Christian Ullner[a,*], Jörg Beckmann[a], Roger Morrell[b]

[a]*Federal Institute for Materials Resarch and Testing, Germany*
[b]*National Physical Laboratory, Teddington, United Kingdom*

Received 10 January 2001; received in revised form 31 July 2001; accepted 6 August 2001

**Abstract**

The standard for advanced technical ceramics ENV 843-4 of 1995 (Vickers, Knoop and Rockwell superficial hardness tests) was validated within the framework of the CERANORM EC-project. The paper reports on depth sensing hardness measurements done for comparison with the other hardness tests. The instrumented indentation test is a modern technique (recent issue ISO/DIS 14577) that has the potential to take into account the specific response of materials in a much better way. An evaluation has been made to establish whether the instrumented hardness technique is a appropriate method for advanced technical ceramics and offers potential for additional applications. 

*Keywords:* $Al_2O_3$; Hardness; Indentation; SiC; $Si_3N_4$; Standards; Testing

## 1. Introduction

Cracking and chipping in the test piece during hardness testing on ceramics are the principal contributions to the high uncertainty in measurement. The instrumented indention test allows an extension to the traditional hardness testing by recording the force and the indentation displacement during the indentation process. The recording option of instrumented indentation tests evokes the question if more reliable results can be achieved?

## 2. Method and analysis

In the instrumented indentation test a pyramidal body [e.g. Vickers pyramid (V) or a Knoop[1] pyramid (K)] is driven into the test piece while indentation force $F$ and penetration depth $h$ are recorded simultaneously.[1,2] Concerning the test pieces, the deformation under load is the sum of the vertical deformation at which indenter contact is made (plastic deformation) and the elastic deformation of the surface at the perimeter of the contact. A penetration depth $h_{max}$ can be registered at a peak load $F_{max.}$. Upon unloading, the elastic deformation recovers and a residual hardness impression is left after removing the indenter. The load versus indentation data plot can be subsequently analysed in the following way. The loading part of the indentation curve characterises the hardness as originally defined by Martens[3] (hardness is the resistance of the material against the penetration by a harder material). A universal hardness[1] can be calculated from the maximum force, $F_{max}$, and maximum penetration depth, $h_{max}$. This type of hardness is named Martens hardness in the new standard ISO/DIS 14577[2]).

$$HM(V) = \frac{F_{max}}{26.43\ h_{max}^2}\ ;\ HM(K) = \frac{F_{max}}{65.38\ h_{max}^2} \tag{1}$$

A Martens hardness based on the slope of the square-root-force against displacement curve can be estimated as follows.[1]

$$HM_s = \frac{\left(\frac{d\sqrt{F}}{dh}\right)^2}{26.43} \tag{2}$$

A plastic hardness value (indentation hardness) has been defined by means of Eqs. (3) and (4).[4] The plastic deformation can be calculated from the separation of the elastic deformation from the total recorded deformation by using the initial unloading slope $S$ [Eq. (3)] or

* Corresponding author. Tel.: + 49-308-104-1914; fax: +49-308-104-1917.
*E-mail address:* christian.ullner@bam.de (C. Ullner).

[1] Knoop indentations are not included in the standards of DIN and ISO.

0955-2219/02/$ - see front matter 
PII: S0955-2219(01)00433-2

from the elastic modulus $E_s$ of the specimen and $E_d$ of the indenter, respectively [Eq. (4)].

$$HVM = \frac{F_{max}}{26.43\left(h_{max} - 0.64\frac{F_{max}}{S}\right)^2}; \quad HKM = \frac{F_{max}}{65.38\left(h_{max} - 0.64\frac{F_{max}}{S}\right)^2} \tag{3}$$

$$HVM = \frac{4HMs(V)}{\left(1+\sqrt{1-12HMs(V)\left(\frac{1-\nu_s^2}{E_s}+\frac{1-\nu_d^2}{E_d}\right)}\right)^2} \tag{4}$$

$$S = \left(\frac{dF}{dh}\right)_{F=F_{max}} \tag{5}$$

$E_d = 1000$ GPa and $\nu = 0.3$ are the elastic constants of the diamond indenter. The slope $S$ originates from the elastic recovery of the deformed material and can be estimated from the unloading curve at the peak load $F_{max}$. The measured slope, $S$, increases with rising Young's modulus of the material and can be used for calculating the indentation modulus $E_{IT}$[4] as an approximation to the Young's modulus.

$$E_{IT} = \left(1-\nu_s^2\right)\left(\frac{5.66\left(h_{max} - 0.64\frac{F_{max}}{S}\right)}{S} - \frac{1-\nu_d^2}{E_d}\right)^{-1} \tag{6}$$

All hardness parameters introduced by the Eqs. (1)–(6) have been calculated for each indentation experiment in the framework of the test.

It should be noted that the factor 0.64 used in the Eqs. (3), (4) and (6) slightly differ from the factors used in the standards.[1,2] The two standards do also not agree in that factor[5]. However, the difference does not affect the conclusions of this paper.

## 3. Hardness machines

Two machines have been used to cover a large range of the penetration depth. The Fischerscope H100 (Helmut Fischer GmbH Sindelfingen) allows measuring the indenter displacement in relation to the specimen surface with a resolution of 3 nm. The force is generated electromagnetically and increased stepwise incrementally up to 1 N. The minimal increment of force is 0.02 mN. Tests have been conducted at a data aquistion rate less than 10 $s^{-1}$ and a force rate of 50 mN $s^{-1}$ after contacting the surface.

The tests up to 10 N have been performed by the HMO100R (Werkstoffprüfmaschinen Leipzig). The machine increases the force continuously and is equipped with a 100 N force transducer working with a resolution of 5 mN. The depth sensing measurement is also related to the specimen surface and a resolution of 5 nm . The tests have been conducted at a data acquisition rate of 6 $s^{-1}$ and a displacement rate at contact of 0.15 μm $s^{-1}$.

Both machines allow measuring the indenter displacement in relation to the specimen surface. Therefore, the machine compliance does not affect the displacement measurement.

## 4. Materials

A broad variety of ceramics was accessible to the instrumented indentation test because the EC-project CERANORM was running at that time. The task 4 of CERANORM mainly dealt with the traditional hardness technique.[6] The project aimed to validate the draft of the CEN standard ENV 843 part 4 to provide in the future more reliable hardness results on advanced ceramics. Reference blocks as well as representative advanced technical ceramics were used for a comprehensive hardness test at 10 different laboratories from Belgium, France, Germany, Italy, and UK.

Advanced ceramics have a very high hardness and a tendency to cracking and chipping. The selection of the indentation force is problematic because the balance between sufficiently large indentations (the high hardness of ceramics gives smaller indentations than in metallic materials) and sufficiently little cracking cannot be found in many cases. Instrumented indentation tests have been evaluated as an alternative to the traditional dead-weight Vickers and Knoop hardness, for ceramics using a single set of materials to check if operator uncertainties can be reduced.

The used materials listed in Table 1 are reference blocks (A, C, D, G, J) and representative commercial products (E, F, H, I, K, L, M). The Table 1 is grouped according to the three widespread materials classes: Silicon nitride, silicon carbide, and aluminium oxide.

Material A is a reference block for HK2 made of hot-isostatically-pressed silicon nitride.[7] The material has a fully dense, very fine-grained, iniform microstructure. Materials C and D are developed for the use as reference blocks with slightly different hardness. The processing by gas-pressure sintering yields an isotropic microstructure for an extented volume.[8] The high quality of reference materials is performed by liquid-phase sintering in the case of silicon nitride (material G). Material J is a result of a certain processing for a product of twice strength and enhanced hardness.[8]

In comparison to the reference blocks the indentation response of commercial ceramics was investigated.

Table 1
Code, trade name and traditional hardness of the materials used in this study

| Code | Source/material code | Type | HV1[a] | HK2[b] |
|---|---|---|---|---|
| A | NIST/SRM 2830 | HPSN | 1580 | 1430 |
| C | IKTS | GPSN | 1470 | 1350 |
| D | IKTS | GPSN | 1480 | 1380 |
| E | Tenmat/Nitrasil R | RBSN | 1020 | 940 |
| F | Lucas-Cookson/Syalon 201 | SiAlON | 1600 | 1410 |
| G | IKTS | LPS-SiC | 2560 | 1960 |
| H | CERAMTEC/CD | SiC | 2650 | 1720 |
| I | CERAMTEC/RK | $Al_2O_3$ | 1890 | 1610 |
| J | IKTS | $Al_2O_3$ | 2120 | 1730 |
| K | Morgan Matroc/VITOX (white) | $Al_2O_3$ | 1990 | 1710 |
| L | Morgan Matroc/SINTOX FA | $Al_2O_3$ | 1530 | |
| M | Morgan Matroc/VITOX (white) + tempered | $Al_2O_3$ | 1800 | 1570 |

[a] HV1—Vickers hardness at 9.81 N.
[b] HK2—Knoop hardness at 19.62 N.

Table 1 lists test pieces of high porosity of 13% (specimens E), high hardness (including a strong tendency to crack) of 2600 HV1 (specimens H), as well as material with fine grain size and low porosity (material K) or medium grain size and medium porosity (material L). To generate a corresponding material with enhanced grain size up to 8 μm material K was tempered at high temperature (material M).

The preparation of specimens was mostly performed by one laboratory to ensure a consistent surface quality. The surface preparation was considered appropriate when the arithmetic mean roughness $R_a$ was less than 0.08 μm. To perform the high quality of reference blocks the arithmetic mean roughness $R_a$ was minimized down to 0.005 μm.

## 5. Behaviour of ceramics

The distinctive features of ceramics, such as an enhanced roughness of the surface due to open pores, porosity in the volume, and multiple phases with different hardnesses, makes hardness measurement more complicated. The penetration of the indenter is additionally influenced by cracking during loading and/or unloading, which occurs more readily at higher forces. However, there are ceramic materials which show near ideal indentation behaviour. A straight line in the square root of the force against displacement plot can be observed according to the rule of geometric similarity in Fig. 1. Each of the ten curves obtained from measurements of hardness reference blocks made of a fully dense fine grained silicon nitride (material A, see Table 1) shows a straight line. They were plotted independently of the initial diamond contact point and closely overlap each other. Deviations from the straight line are observed only near the contact point for the silicon nitride-based Syalon (material F, see Table 1), this material containing approximately 13% by volume of fine pores. This effect appears to be caused by the surface roughness including pores at the surface.

By comparison, Fig. 2 shows indentation curves up to 10 N for blocks made from an other type of silicon nitride, the porous reaction-bonded form (material E). Each curve in Fig. 2 is distinctly influenced by the local microstructure where indentation has taken place. The scatter of the slope, as well as the position of the different curves is much bigger than in the denser finer-grained, more homogeneous material. The presence of pores and cracking affect the shape of the indentation such that the usual analysis procedure seems inappropriate to get reasonable results.

## 6. Results on commercial ceramics of $Si_3N_4$, SiC, and $Al_2O_3$

Figs. 3–5 illustrate the normalized hardness results gained from the instrumented indentation tests on different advanced ceramics. All instrumented hardness values have been calculated according to Eqs. (1)–(5) and subsequently normalized by the traditional Vickers

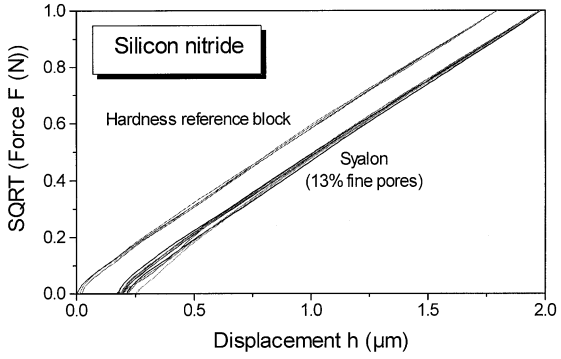


Fig. 1. Ideal indentation behaviour of hardness reference blocks (specimen A). A small deviation near the contact point can only be observed in the case of Syalon (material F).

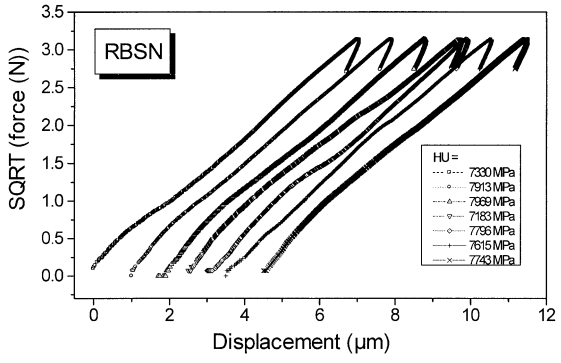


Fig. 2. Stochastic indentation behaviour of Nitrasil R (RBSN, material E).

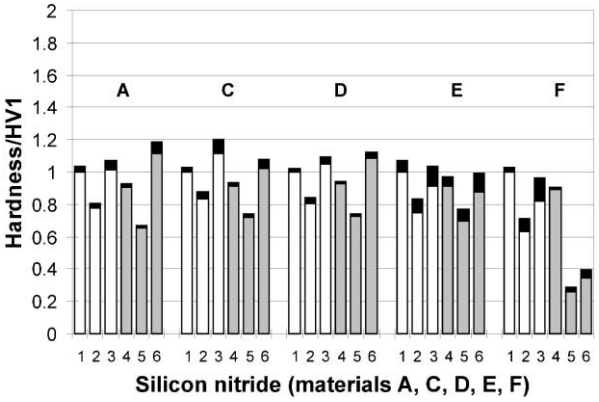


Fig. 3. Comparison of the three hardness numbers 1—HV, 2—HM(V), 3—HVM (white bars, Vickers indenter) and the three hardness numbers 4—HK, 5—HM(K), 6—HKM (gray bars, Knoop indenter) for Silicon nitride. The indentation force is 9.81 N. All hardness numbers have been normalized by the traditional Vickers hardness HV1. The black part on the top of the bar is the one-sided standard deviation of the individual test.

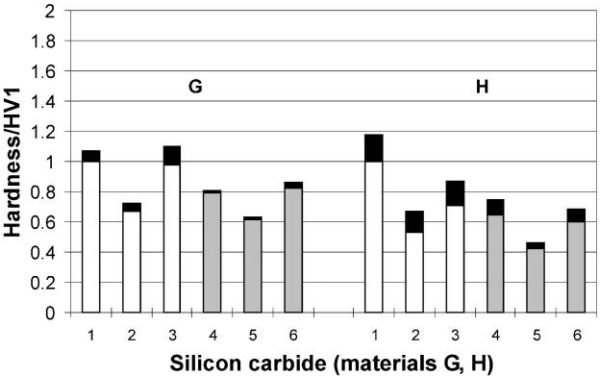


Fig. 4. Comparison of the three hardness numbers for silicon carbide. See Fig. 3 for further description.

hardness HV1. The black part on the top of each bar stands for the one-sided standard deviation of the individually performed test series. Additionally, the coefficient of variation, COV, has been calculated. COV is the ratio of standard deviation to the normalized hardness, expressed as a percentage. The results on silicon nitride are shown in Fig. 3. With exception of one case, the COVs of the instrumented indentations exceed the value achieved by the traditional techniques. The ranking between the hardness parameters does not change in the case of the fully dense reference materials (materials A, C and D) unlike for the commercial engineering ceramics (materials E and F). The calculated "plastic" hardness HVM (the third bar in each group) corresponds to the conventional Vickers hardness (first bar of each group) only for specimens qualified for reference materials (A, C, D). The two hardness values become significantly different from each other for commercial engineering materials with higher inherent porosity (E, F). The COV

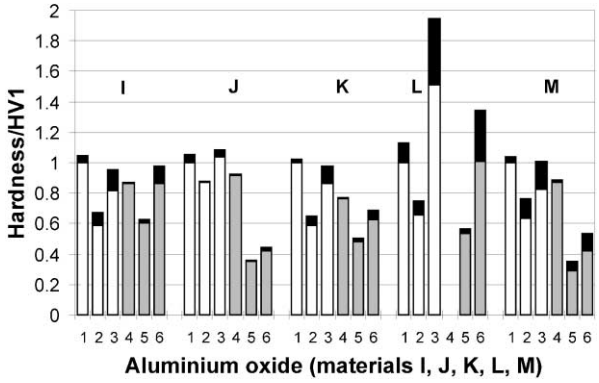


Fig. 5. Comparison of the three hardness numbers for aluminium oxide. See Fig. 3 for further description.

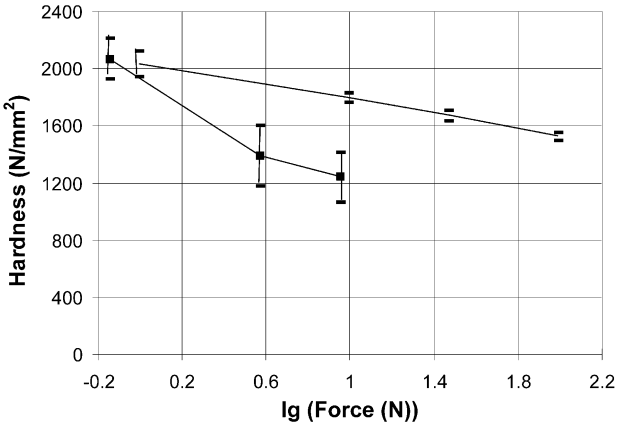


Fig. 6. Force dependence of the traditional hardness HV and the plastic hardness HVM for the material M. The standard deviations are indicated by error bars.

Table 2
Comparison of the Young's moduli (indentation moduli) determined from Eq. (4), loading curve, and from Eq. (6), unloading curve

| Material | HV1[a] | | $HM_s10$[b] | | $E_{fit}$ after Eq. (4) (GPa) | $E_{IT}$ after Eq. (6) (GPa) | |
|---|---|---|---|---|---|---|---|
| J | 1580 | 2%[c] | 14000 | 2% | 350 | 410 | 8% |
| K | 1990 | 4% | 9500 | 19% | 150 | 310 | 11% |
| M | 1800 | 4% | 8900 | 28% | 140 | 400 | 29% |

[a] HV1 is the Vickers hardness (in kp $mm^{-2}$) at 1 kg [6].
[b] $HM_s10$ is the Martens hardness (in N $mm^{-2}$) for the range from 5 to 10 N.
[c] The values in % are the corresponding coefficients of variation (COV).

of the HV and HVM are so high that their correspondence can no longer be confirmed. Although HV equals in some cases HVM within the error bars, the porosity produces the higher standard deviation of the HVM value in the same manner as for samples with high surface roughness. Because the cracking is influenced sensitively

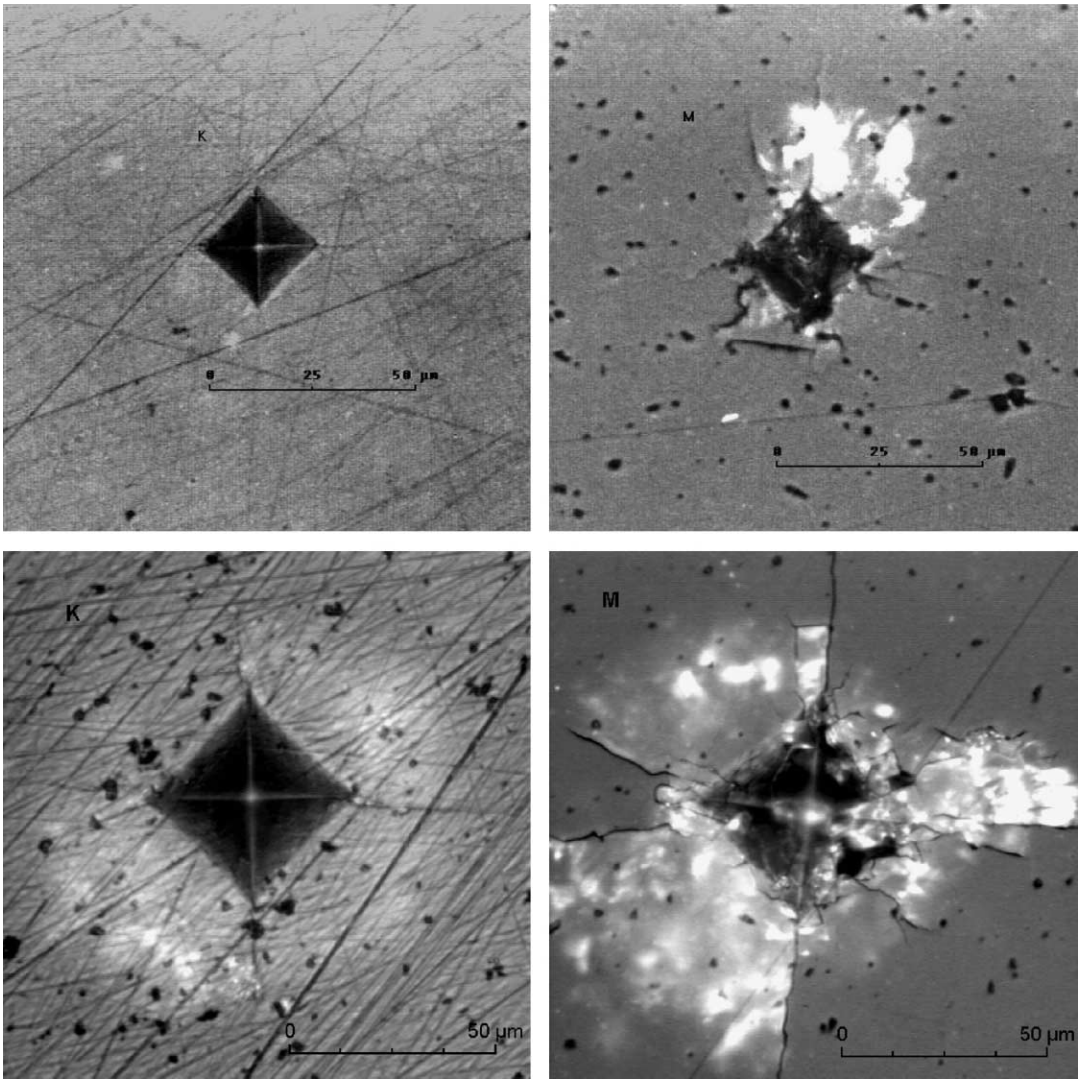


Fig. 7. Vickers indentation at 9.81 N (above) and 29.43 N (below) on specimen K (aluminium oxide with smaller grain size, left) and M (aluminium oxide with enhanced grain size, right).

by the geometry of the indenter, the response of Knoop hardness is different from that of Vickers hardness.

Similar results were found for SiC (Fig. 4). The HM values of silicon carbides have higher COV's than those of silicon nitrides. Nevertheless, although an increasing standard deviation of HM can be observed, the plastic hardness approximately equals the traditional hardness for the reference quality specimen (G). The difference between HVM and HV becomes even more visible in material H than in material F. This result points to the fact that non-elastic surface deformation outside the indenter contact has occurred (see Section 7).

The last group of materials is $Al_2O_3$, and the results are shown in Fig. 5. The response is no different to the other material types. The reference type specimen J yields results with relatively small scatter. HVM and HV are equivalent quite well. With increasing grain size and porosity the scatter is rising and the elastic response becomes confusing (see Section 7). Again, the results of Knoop hardness differ from those of Vickers hardness.

## 7. Effects of force and cracking

Access to information about the force dependence of the hardness is a benefit of the depth sensing hardness experiment. The force dependence of the plastic hardness HVM calculated from the Martens hardness $HM_s$ according to Eq. (4) is compared with the force dependence of the traditional hardness HV for the material M in Fig. 6 (HV from[6]). The force dependence of HVM is more pronounced than in the case of the traditional hardness. It is based on rising additional displacement caused by the compliance of the indenter shaft or by the changed elastic response of the material. Because the compliance of the indenter shaft is only about 0.02 µm

$N^{-1}$ the rising elasticity of the material seems to influence the Martens hardness. In fact, the agreement between HVM and HV at 0.1 N in Fig. 6 could only be satisfied by employing a fitting value, $E_{fit} = 240$ GPa, rather than the value of $E_s = 400$ GPa measured by the traditional technique. However, there is a contradiction to the indentation modulus, $E_{IT} = 400$ GPa, determined from the initial unloading slope of the same indentation test on material M (Table 2). Enhanced cracking is the explanation for this contradiction (Fig. 7).

Fig. 7 shows the impressions generated by the Vickers indenter at 9.81 and 29.43 N into specimen K (aluminium oxide with smaller grain size) and M (aluminium oxide with enhanced grain size). The photographs indicate cracking of the microstructure in the surroundings near the residual indent. This observation is more pronounced on specimen M than for specimen K.

The elastic parameters fitted by the comparison between HV1 and $HM_s10$ (named $E_{fit}$) or determined from the initial unloading slope ($E_{IT}$) of ten indentation runs are gathered in Table 2 for the aluminium oxide ceramics J, K, and M. While the indentation test on material J with the quality of reference block (dense, non-porous ceramic material) gives corresponding values of $E_{fit}$ and $E_{IT}$ differences can be seen for the commercial aluminium oxide ceramics K and M. As shown in Fig. 7 the cracking of the coarse grain material M is extended in the region outside the impression. This region determines the elastic portion of Martens hardness. During the force application the additional displacement (originally assumed to be elastic) is increased by cracking of the microstructure near the residual indent as documented in Fig. 7. During the following force removal the elastic robound of the material is less than expected because the microstructure is disturbed. Therefore, $E_{IT}$ does not decrease while $E_{fit}$ decreases from material K to M (Table 2). Because cracking is a stochastic event the scatter is increased in the order J, K, and M.

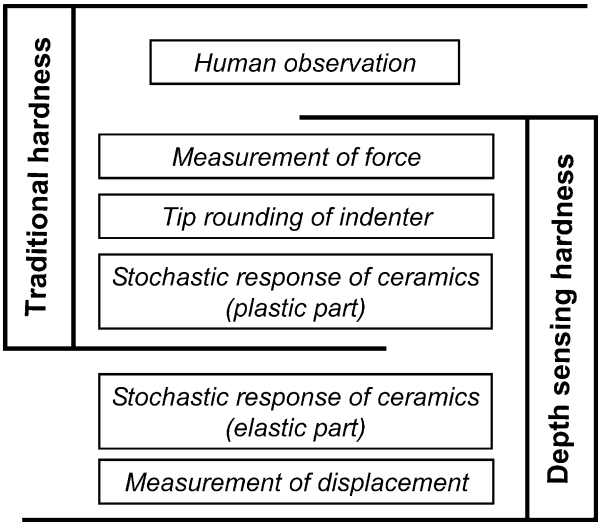


Fig. 8. Contributions to the uncertainty in measurement for the traditional and depth sensing hardness (instrumented indentation test).

This result could also be confirmed for the materials H and I. The contribution of non-elastic deformation due to the indentation clearly increases with enhanced force in relation to the plastic part quantified as the visible residual indentation. In contradiction to the loading curve, the measured initial slope of unloading curve, $S$, is higher than the expected value

## 8. Discussion and conclusion

The instrumented hardness test did not reliable match the traditionally estimated hardness in contrast to initial expectations. To summarise the reasons for the different results, contributions to the overall uncertainty have been considered and sketched schematically in Fig. 8. The left side of the scheme shows the contributions to uncertainty in the traditional hardness test. The uncertainty in the length measurement performed by human observer has been considered to be particularly important in the traditional technique. On the right side of Fig. 8 are grouped the contributions to uncertainty in the instrumented hardness test. A higher total uncertainty with this test could be observed even though it eliminates the observer. The uncertainty of the hardness appears to be mainly related to the stochastic response of ceramic materials during surface deformation. The stochastic surface response can result in different HM value ranking, and increases the uncertainty to a level that is greater than the uncertainty involved with traditional human observation. Surface deformation outside the indenter can be considered to be inelastic due to cracking for many typical ceramics. It affects the slope of loading and unloading curve in a different way.

The instrumented hardness technique allows the evaluation of the elastic response in the micro-range after indenting by using the initial slope of the unloading curve. That is why depth-sensing hardness measurements are more appropriate than traditional methods to study the characteristic indentation response of ceramics. However, this research has shown that it does not presently provide a technique for reducing the error levels associated with visually derived measurements if chipping and cracking can occur during the indentation test. Therefore, more work is needed to exploit effectively the potential of the instrumented indentation test for advanced ceramics.

## Acknowledgements

The financial support of the European Commission under Contract Number SMT4-CT96-2078 is gratefully

acknowledged. The authors wish to thank Dr. Thomas Reich, Fraunhofer-Institut für Keramische Technologien und Sinterwerkstoffe, Dresden, for supplying the ceramic reference blocks.

## References

1. DIN 50359 Universalhärteprüfung, Teil 1: Prüfverfahren, Beuth-Verlag, October. 1997 (English issue available).
2. ISO/DIS 14577: Instrumented indentation test for hardness and other materials parameter; April 2000.
3. Martens, A., *Handbuch der Materialienkunde für den Maschinenbau*. Springer, Berlin, 1898.
4. Weiss, H. J., Universalhärte. *Materialprüfung*, 1997, **39**(9), 368–373.
5. Ullner, Ch. and Wehrstedt, A., Martenshärte, Eindringhärte oder Eindringmodul ermitteln—instrumentierte Eindringprüfung nach ISO/DIS 14577. *Härtetechnische Mitteilungen HTM*, 2001, **56** in press.
6. Ullner, C., Germak, A., le Doussal, H., Morrell, R., Reich, T. and Vandermeulen, W., Hardness testing on advanced technical ceramics. *J. Eur. Ceram. Soc.*, 2000, **21**, 439–451.
7. Gettings, R. J., Quinn, G. D., Ruff, A. W. and Ives, L. K. Development of ceramic hardness reference materials. Proc. 8th World Congress of Ceramics CIMTEC, July 1994, Florence, Italy, Section SM, Poster 02.
8. Reich, T., Ullner, C. and Polzin, T., Referenzproben für die Härteprüfung an Hochleistungskeramiken. *Härteprüfung*, 2001, **43**, 108–112.